InGaAs SCHOTTKY BARRIER MIXER DIODES FOR MINIMUM CONVERSION LOSS AND LOW LO POWER REQUIREMENTS AT TERAHERTZ FREQUENCIES *

U.V. Bhapkar, T.A. Brennan and R.J. Mattauch

Semiconductor Device Laboratory
Department of Electrical Engineering
The University of Virginia
Charlottesville, VA 22903-2442

ABSTRACT

This paper presents a theoretical investigation of the conversion loss of mixers using InGaAs Schottky barrier diodes as well as experimental findings on these diodes.

The conversion loss study is based on a multi-port mixer analysis developed by Held and Kerr. This analysis requires a knowledge of the embedding impedance presented to the diode, as well as the diode parameters, such as the series resistance, the junction capacitance, and the current-voltage characteristic. We have performed an analysis of the current-voltage characteristics of Schottky diodes based on the work of Crowell, Chang and Sze. This model considers the effects of electron tunneling and image force lowering of the barrier. The conversion loss studies indicate that InGaAs diodes will offer comparable conversion performance to that of GaAs diodes with DC bias. The calculations also show that non-biased InGaAs diodes are expected to require about one-sixteenth of the LO power required by non-biased GaAs diodes. We also present conversion loss predictions of sub-harmonically pumped, anti-parallel diodes, and show that to achieve minimum conversion loss, $In_{0.53}Ga_{0.47}As$ diodes will require one-eighth of the power required by GaAs diodes.

Several batches of back-contacted InGaAs diodes with indium mole fractions of 0.2 and 0.3 have been fabricated on GaAs substrates. The fabrication procedure used to make the InGaAs diodes is similar to that used for high frequency GaAs devices. The DC testing indicates that the InGaAs diode performance compares favorably with that of the best GaAs devices in terms of the ideality factor, parasitics, and the breakdown voltage. These devices had a lower turn-on voltage than conventional GaAs devices, as expected.

* This work was supported in part by NASA through the University of Michigan Space Terahertz Technology Center under grant Z-25251, and by the National Science Foundation under grant ECS-8720850-02.

I. Introduction

GaAs Schottky diodes are frequently used as mixer elements in heterodyne receivers for the few hundred gigahertz to 1 terahertz frequency range. At present a major limitation of these devices is the difficulty in obtaining sufficient local oscillator (LO) power from solid state sources at these frequencies. One solution to this problem is to use sub-harmonically pumped, anti-parallel diode pairs. This will halve the frequency at which the LO power is needed to a range where obtaining sufficient LO power is less of an obstacle. GaAs diodes can be used in such a configuration, but unfortunately, they require a significant DC bias or high LO power for optimum conversion performance, and it is very difficult to bias diodes used in this manner. To solve this problem, InGaAs has been proposed as a material for use in sub-harmonically pumped, anti-parallel diode structures. Schottky barriers formed from $In_xGa_{1-x}As$ have a height that decreases with increasing indium mole fraction. The Schottky barrier height is critical in mixer operation because it determines the turn-on voltage of the diode. A diode with a lower turn-on voltage requires less DC bias to reach its optimal operating range. An added benefit of using InGaAs is its mobility, which is superior to that of GaAs. This is important because the high mobility will lead to a lower series resistance, which is a parasitic that lowers the overall conversion efficiency of the diode.

This paper presents a report on progress towards the goal of developing an InGaAs Schottky diode mixer having superior performance and LO power requirement for use at frequencies up to 1 THz. The effort thus far has consisted of both theoretical and experimental work. The theoretical work has focused on predicting InGaAs diode parameters as well as the conversion efficiency of mixers using these diodes. The experimental work has focused on perfecting the fabrication sequence of InGaAs diodes formed on GaAs substrates.

Section II of this paper presents the diode models that have been used in the conversion loss analysis. A major effort of our research has been the development of a computer program that calculates the current-voltage characteristics of Schottky diodes while taking into consideration the quantum mechanical reflection of electrons at the Schottky barrier. This analysis, based on the work of Crowell, Chang, and Sze, also takes into consideration the image force lowering of the Schottky barrier [1,2]. A new model of the RF series impedance is also outlined [3]. This model considers the structure of diodes with epitaxial layers, and automatically incorporates into the calculation high frequency phenomena such as the skin effect and charge-carrier inertia. Section III presents the results of conversion loss calculations of both single diode and anti-parallel GaAs and InGaAs diodes. These calculations are based on a multi-port mixer analysis developed by Held and Kerr [4,5]. We have used a modified version of a computer program by S. Maas to perform the analysis [6]. The modifications to the program include the use of our own current-voltage analyses, rather than the standard thermionic-emission model. This analysis requires a knowledge of the embedding impedance presented to the diode, as well as the diode parameters discussed in Section II. Section IV presents experimental work. The fabrication technology which produces InGaAs diodes with predictable, desirable mixer characteristics is discussed. The DC characteristics of four batches of InGaAs diodes are reported, along with those of typical GaAs diodes for comparison. The InGaAs devices compare well with the GaAs diodes even though their fabrication procedure has not yet been optimized. Section V concludes this paper and indicates areas of present and future work.

II. Diode Models

The diode parameters needed for the implementation of the conversion loss analysis are:

A. the Schottky barrier height,
B. the junction capacitance,
C. the RF series resistance, and
D. the current-voltage characteristic.

Because the study of InGaAs Schottky diodes is in its infancy, the experimental base to provide some of these parameters, particularly the last two, is inadequate. Therefore, to obtain valid predictions of the conversion loss, we first performed new, more accurate calculations of the RF series impedance and the current-voltage characteristic.

A. Schottky Barrier Height

The Schottky barrier height of $In_xGa_{1-x}As$ as a function of the mole fraction, x, is given by the following empirical formula [7]:

$$\phi_B = 0.95 - 1.90x + 0.90x^2. \tag{1}$$

The Schottky barrier height, given by (1), is plotted in Fig. 1, and decreases very rapidly with increasing indium mole fraction. This is of critical importance to mixer operation because the Schottky barrier height determines the diode turn-on voltage, and diodes with a low turn-on voltage may require the application of less bias and/or LO voltage. Thus, InGaAs diodes are expected to require less LO power in comparison to that required by GaAs diodes. Also, InGaAs diodes will improve the performance of mixer configurations in which it is not possible to bias the diodes, such as in sub-harmonically pumped, anti-parallel pairs.

B. Junction Capacitance

The junction capacitance, C_j, is a parasitic element that affects the conversion loss of the diode, and is given by

$$C_j = \frac{C_{jo}}{(1-V/\phi_B)^{1/2}}, \tag{2}$$

where C_{jo} is the zero-biased junction capacitance. In whisker-contacted diodes, C_{jo} is given by [8]

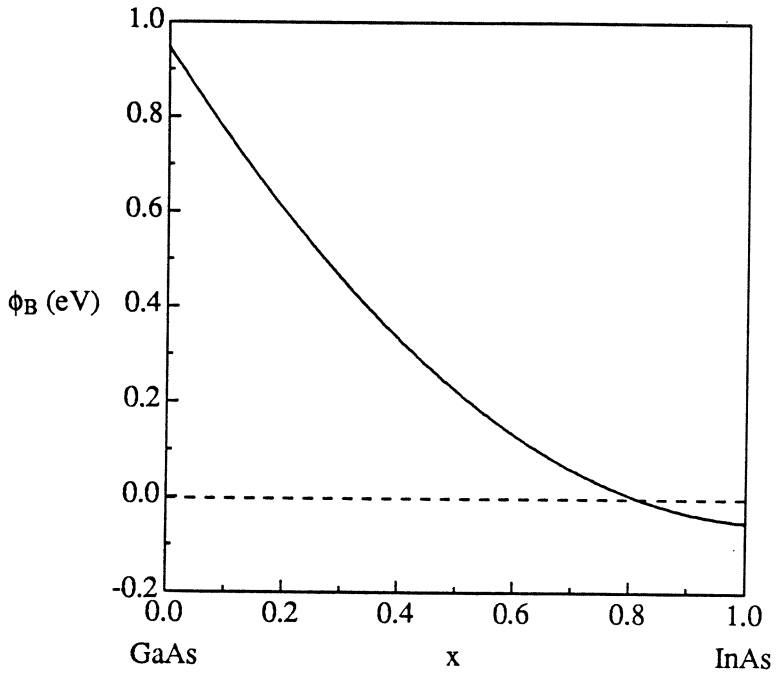

Figure 1. Schottky barrier height of $In_xGa_{1-x}As$ as a function of indium mole fraction.

$$C_{jo} = \frac{\varepsilon A}{W} + \frac{3\varepsilon A}{2a}, \tag{3}$$

where ε is the permittivity of the semiconductor, a is the anode radius, A is the anode area, and W is the zero-biased depletion depth, given by

$$W = \left[\frac{2\varepsilon\phi_B}{qN}\right]^{1/2}, \tag{4}$$

where N is the doping concentration in the region below the anode. The second term in (3) is due to the fringing of the electric field near the anode edges.

C. RF Series Impedance

The RF series impedance of Schottky barrier diodes is a complicated function of the frequency, and no analytic formulae of sufficient accuracy are available. Dickens' formula of the series impedance has commonly been used [9], but it is accurate only for simple diodes without epitaxial layers and with the ohmic contact encircling the diode chip. Real Schottky diodes usually have epitaxial layers and have the ohmic contact on the back or on top of the chip. In addition, the formula loses accuracy at frequencies greater than several hundred gigahertz. Therefore, we have developed a finite difference calculation of the RF series impedance that considers these factors [3]. These computer programs obtain the solution to the electromagnetic field over the entire diode chip, which, for ease of calculation, is assumed to be cylindrical. The actual diode chip of the planar structure, as shown in Fig. 2, is rectangular, and the whisker-contacted structure, as shown in Fig. 3, is square-shaped. Use of the cylindrical approximation causes only a small error in the series impedance calculation of the whisker-contacted chip. For the planar diode structures our finite difference calculations offer a less accurate prediction of the series impedance because it models the ohmic contact as entirely encircling the anode. In an actual chip, the ohmic contact occupies only about half of the wafer's top surface. In spite of these simplifications, our model is useful for comparing the series impedance of different diodes. Figures 4 and 5 depict two-dimensional cross sections of the current contours within whisker-contacted and planar diodes, respectively.

The series impedance of course depends on the electron mobility μ of each layer in the diode. We have proposed the following empirical formula for the electron mobility at 300 K, expressed in $cm^2V^{-1}s^{-1}$:

$$\mu = \frac{7250(1 + 2.9x)}{1 + 1.6\times10^{-9}N^{1/2}}, \tag{5}$$

where N is the doping concentration of the semiconductor in cm^{-3}. This formula was obtained from experimental data on the mobility of doped GaAs [10] and InAs [11], and assumes a linear dependence of the mobility on the indium mole fraction. The predicted mobility agrees with a simulation of the mobility of $In_{0.53}Ga_{0.47}As$ doped at 10^{18} cm^{-3} [12]. Experimental findings indicate that the mobility of $In_{0.53}Ga_{0.47}As$ on lattice matched InP is somewhat lower than predicted by (5), but is significantly greater than that of GaAs [13]. This will lead to lower series impedance in devices using $In_{0.53}Ga_{0.47}As$ on lattice matched InP than in standard GaAs devices. However, devices with InGaAs epilayers on GaAs substrates will have strained lattices, which may affect the mobility of the InGaAs layer.

The thickness of the epilayer also affects the series impedance. The epilayer of Schottky diodes is usually made to approximate the zero-biased depletion width, given by (4). Due to its dependence on the Schottky barrier height, the depletion width decreases with increasing indum mole fraction. Therefore, it is possible to fabricate InGaAs diodes with thinner epilayers than those in GaAs diodes, leading to lower series impedance in these devices.

D. Current Voltage Characteristic

A highly accurate model of the current voltage characteristic of the Schottky diode is essential to obtain a reasonable estimate of the conversion loss. The most frequently used models, such as Bethe's thermionic emission model [14] and Padovani and Stratton's field-thermionic emission model [15], are

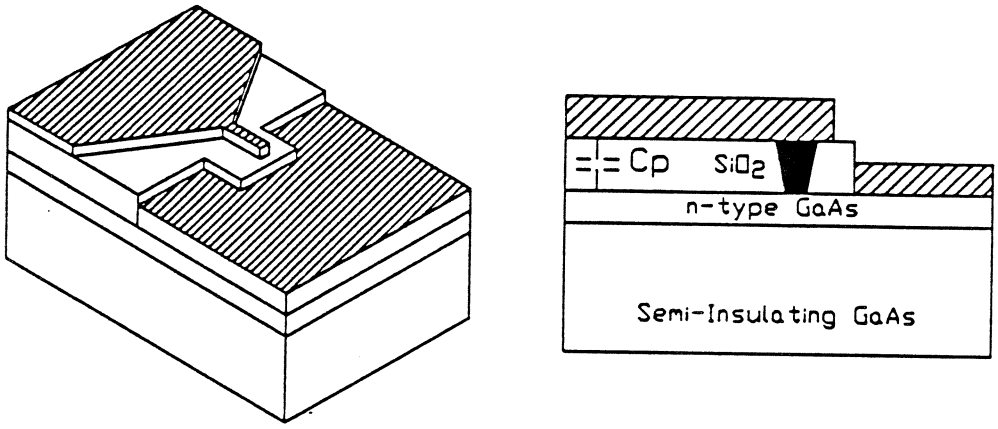

Figure 2. Planar diode chip.

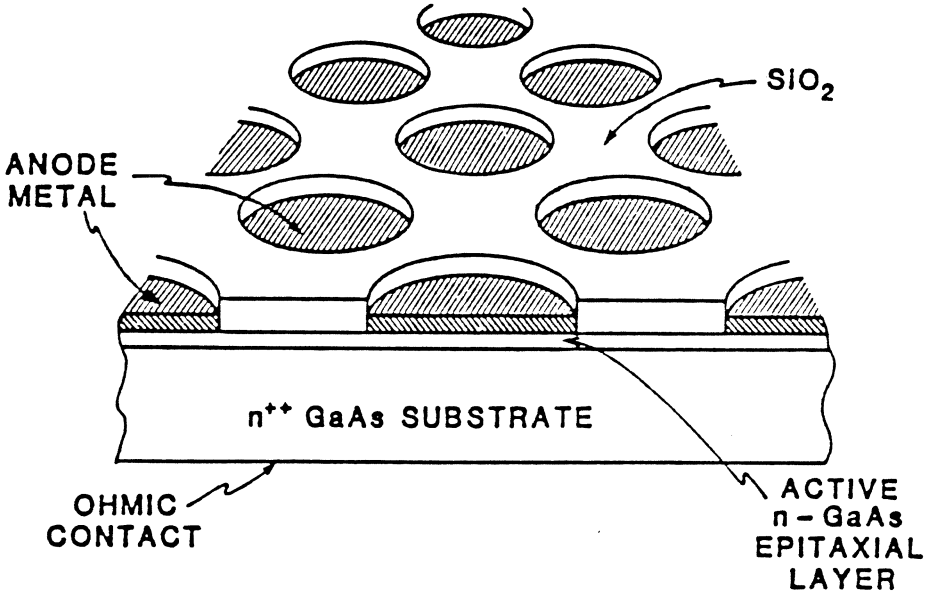

Figure 3. Whisker-contacted diode chip.

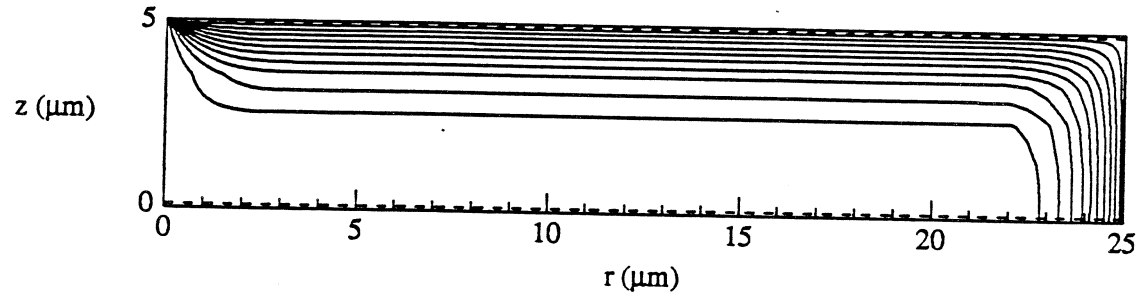

Figure 4. Current contours within whisker-contacted diode chip. Each line represents 10 percent of the total current.

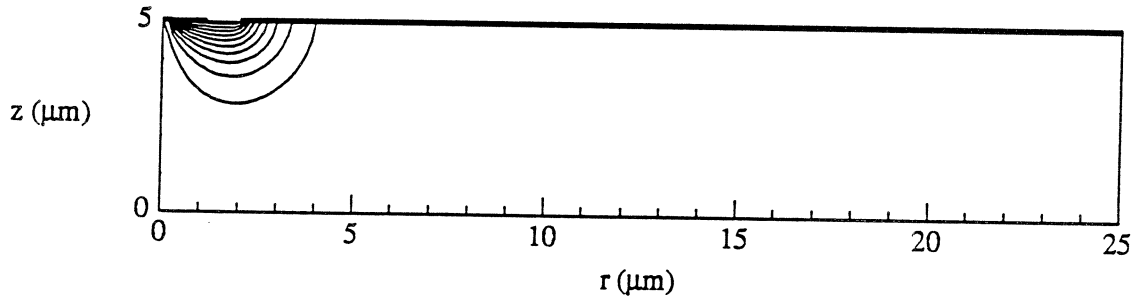

Figure 5. Current contours within planar diode chip.

either insufficiently accurate, or are applicable only in a limited voltage range. We therefore use a more sophisticated model similar to that of Crowell, Chang and Sze [1,2].

According to the thermionic emission model, the diode I-V characteristic is given by

$$I = I_{sat}\exp(V/V_o) \tag{6}$$

where I_{sat} is the saturation current and V_o is the inverse slope parameter, given by

$$V_o = \eta\frac{kT}{q}, \tag{7}$$

where η is the ideality factor. The ideality factor is an attempt to match the observed I-V characteristics of Schottky diodes with the thermionic emission model. The saturation current is expressed as

$$I_{sat} = ART^2\exp(-\phi_B/V_o), \tag{8}$$

where A is the anode area, R is the Richardson constant, and T is the temperature. The Richardson constant is given by

$$R = \frac{4\pi q m^* k^2}{h^3}, \tag{9}$$

where k is Boltzman's constant, h is Plank's constant, and m^* is the electron effective mass in the semiconductor. The electron effective mass in $In_xGa_{1-x}As$ varies with the indium mole fraction. We used a linear fit between the InAs and GaAs electron effective masses, given by

$$m^* = (0.067 - 0.044x)\, m_e, \tag{10}$$

where m_e is the free electron mass. Because the dominant factor in the saturation current is the barrier height, the saturation current increases very rapidly with the mole fraction. An important question therefore is whether the greater saturation currents of InGaAs diodes will decrease their conversion performance relative to that of GaAs diodes.

Due to various other phenomena, the actual I-V characteristic of a Schottky diode is more complicated than predicted by (6). Electron tunneling, for example, is an important effect, and has been investigated by Padovani and Stratton [15] and Crowell, Chang and Sze [1,2]. Chang and Sze's model also includes image force lowering of the Schottky barrier, and is the most sophisticated model available.

Padovani and Stratton have obtained analytic formulae for the case of thermionic-field emission, in which most of the emitted electrons have an energy greater than the Fermi energy, but tunnel through the barrier. These equations have been found to accurately predict the I-V characteristics at low and intermediate applied bias, but fail at bias voltages close to or exceeding the barrier voltage; in the latter regime, the dominant transport mechanism is not tunneling, but thermionic emission. Their method therefore cannot be used to obtain a continuous I-V relationship over the entire operating range of a Schottky diode mixer, from negative applied voltage to forward voltage exceeding the barrier voltage. The method of Crowell, Chang, and Sze resolves this deficiency, and also allows accurate consideration of image force effects.

Crowell and Sze [1] have developed a method that comprehensively calculates the transmission probability of an electron through the Schottky barrier. The model calculates the quantum mechanical transmission coefficient T(E,V) as a function of the electron energy E for a particular applied bias V. The method is applicable for both tunneling (in which the electron energy is less than the barrier height) and thermionic emission (in which the electron energy is greater than the barrier height). The model is based on a solution of Schrodinger's equation in one dimension,

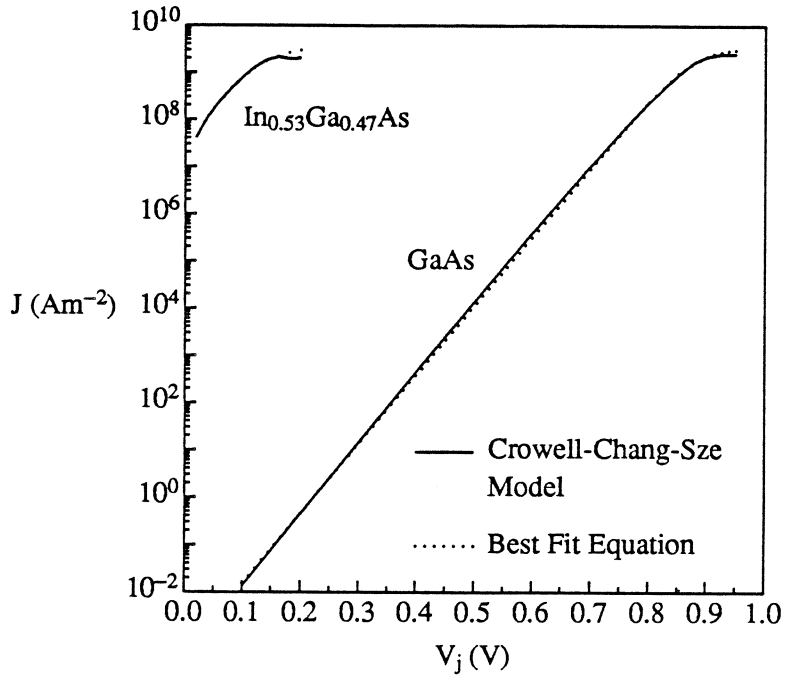

Figure 6. Predicted current-voltage characteristics of GaAs and $In_{0.53}Ga_{0.47}As$ Schottky diodes.

$$-\frac{\hbar^2}{2m}\frac{d^2\Psi}{dx^2} + V(x)\Psi(x) = E\Psi(x), \tag{11}$$

which is solved by imposing continuity relationships on the wavefunction $\Psi(x)$ and $\frac{1}{m}\frac{d\Psi}{dx}$ at the edge of the depletion region and at the metal-semiconductor boundary. V(x) is the potential in the depletion region, given by

$$V(x) = q\phi_B - \frac{q^2N}{\varepsilon}\left[Wx - \frac{x^2}{2}\right] - \frac{q^2}{16\pi\varepsilon x}. \tag{12}$$

The first term represents the potential due to the Schottky barrier, the second term is the potential in the depletion region, and the last term is due to the image force. After obtaining the wavefunction, we calculate the quantum transmission coefficient by comparing the probability density of the transmitted to the incident current. The probability current density is given by

$$j = \frac{q\hbar}{2im}\left[\Psi^*\frac{d\Psi}{dx} - \Psi\frac{d\Psi^*}{dx}\right]. \tag{13}$$

Chang and Sze have developed a method that incorporates Crowell's calculation of the transmission coefficient to obtain the diode I-V characteristic [2]. The total current density in this analysis is given by

$$J(V) = \frac{RT}{k}\int_0^\infty T(E,V)\,[F_s(E,V) - F_m(E)]\,dE, \tag{14}$$

where F_s and F_m are the Fermi-Dirac distributions in the semiconductor and the metal, respectively. The above expression considers the current in both directions, and as noted earlier, considers the tunneling current as well as the current due to electrons traveling over the barrier. The calculation requires T(E,V) to be calculated at several hundred discrete energies for each applied voltage, in order to obtain reasonable accuracy. The only drawback to this algorithm is that several million floating point operations are required to generate each (I,V) pair. This model, as well as the other models mentioned, assume thermal equilibrium electron distribution functions. At very high applied bias, this assumption may not be reasonable.

Figure 6 shows the I-V characteristics of various Schottky diodes as predicted by the preceding algorithm. The logarithm of the current, plotted versus the applied bias, has a fairly constant slope at low bias, but the slope decreases as the applied bias approaches the barrier voltage. Therefore, it is not sufficient to characterize the Schottky I-V relationship by a single parameter V_o; the reduction of the slope at high applied voltage must be taken into consideration. This is particularly important in mixer diodes that are operated at high bias and/or LO voltage, which is usually done in order to obtain the lowest possible conversion loss.

Rather than input the discrete (I,V) pairs into the conversion loss program, we used the following best-fit equation:

$$I(V) = \frac{1}{\frac{1}{I_{max}} + \frac{1}{I_{sat}[\exp(qV/\eta kT) - 1]}}, \tag{15}$$

where the parameters I_{max}, I_{sat}, and η were obtained from a fit to the I-V output of the Crowell-Chang-Sze analysis. As seen in Fig. 6, a fairly good fit can be obtained.

Figure 7 shows a comparison of the I-V characteristics obtained from this model with experimental data collected on an InGaAs diode, SDL33/1/5. The area of the diode was deduced from the measured capacitance along with other diode parameters, using (3). The indium mole fraction was deduced by matching the magnitude of the current at low applied voltage to that predicted by the theoretical model. The value of the deduce indium mole fraction was lower than that specified by the material supplier. We speculate that this discrepancy may be due to strain on the non-latice matched InGaAs of this sample. The strain may increase the energy gap and the Schottky barrier height of the semiconductor, and

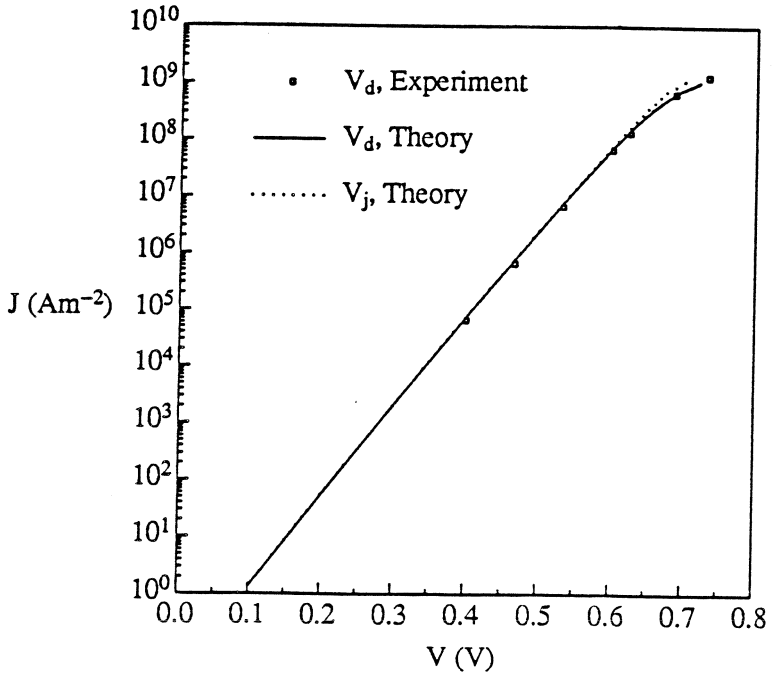

Figure 7. Theoretical and experimental current-voltage characteristics of InGaAs diode SDL 33/1/5. The theoretical calculations assume x = 0.11, R_s = 13.2 Ω, and anode diameter = 1.3 μm.

therefore make it behave as InGaAs with a smaller amount of indium. An excellent fit between theory and experiment was obtained throughout the voltage range. Apparently, deviations from thermal equilibrium statistics are not significant for this diode in the voltage range considered.

III. Conversion Loss Analysis

The conversion loss calculations that we have performed are based on the so-called multiple reflection algorithm developed by Held and Kerr [4,5]. A Pascal language computer program by S. Maas, known as DIODEMX, was used to perform the calculations [6]. Our only modification to the program was to use the I-V model described above, rather than the thermionic emission model.

A. Theory

The analysis discussed here is based on the assumption of a large signal LO source, upon which is superimposed a small signal RF. The time-dependent conductance of the diode is determined through a non-linear analysis known as the large signal algorithm, through use of the multiple reflection algorithm. The diode waveform is then resolved into the small signal admittance, represented in the frequency domain through its Fourier coefficients, which in turn is used to calculate the conversion performance of the diode. This analysis assumes a knowledge of the diode parameters as well as the embedding impedances.[1]

[1] The discussion in this section follows Maas, *Microwave Mixers*, to which the reader is referred for more details [6].

1. Large Signal Analysis

The mixer equivalent circuit is described by a series of loop equations at the mixing frequencies ω_n:

$$\omega_n = \omega_o + n\omega_{LO}, \tag{16}$$

where

$$n = -N, \cdots -2, -1, 0, 1, 2, \cdots N.$$

The value of N is necessarily finite for computation purposes, although in theory the current and voltage exist at an infinite number of harmonics. The loop equations are

$$V_{sn} - Z_{sn}I_{dn} - V_{dn} = 0, \tag{17}$$

where

$$V_{s0} = V_{DC} \tag{18}$$

and

$$V_{s1} = V_{LO}, \tag{19}$$

and all other V_{sn} are equal to zero. I_{dn} and V_{dn} are the diode current and voltage at the n^{th} harmonic, which are obtained through use of the multiple reflection algorithm, which we shall not describe here [4,5]. Z_{sn} is the large-signal embedding impedance presented to the diode at the n^{th} harmonic. The available LO power, P_{LO}, is given by

$$P_{LO} = \frac{V_{LO}^2}{8\,\mathrm{Re}(Z_{s1})}, \tag{20}$$

where Z_{s1} is the LO source embedding impedance.

2. Small Signal Analysis

The small signal voltage and current of the diode may be represented by

$$v(t) = \exp(j\omega_o t) \sum_{-N}^{N} V_n \exp(jn\omega_{LO}t) \tag{21}$$

and

$$i(t) = \exp(j\omega_o t) \sum_{-N}^{N} I_n \exp(jn\omega_{LO}t). \tag{22}$$

The time varying impedance may be represented by its Fourier series

$$z(t) = \sum_{-N}^{N} Z_n \exp(jn\omega_{LO}t), \tag{23}$$

where Z_n includes the series resistance R_s as well as the Fourier coefficients of the junction conductance and capacitance of the diode. Using Ohm's Law, these equations may be written in matrix form as

$$\mathbf{V} = \mathbf{Z}\,\mathbf{I}, \tag{24}$$

where **I**, **V**, and **Z** are matrices consisting of the coefficients discussed above.

Calculation of the conversion performance requires that the 2N + 1 port network discussed above be converted into a two port network consisting of the RF and the IF ports, at frequencies ω_1 and ω_0, respectively. This is achieved by modifying **Z** by adding the embedding impedances Z_{en} to its diagonals. The resulting augmented matrix, $\mathbf{Z}^a$, is inverted to form an admittance matrix, **Y**. Finally, all voltages, except at the RF and IF frequencies, are set to zero.

The conversion loss L of the mixer is defined as

$$L = \frac{P_{IF}}{P_{RF}} = 4|Y_{01}|^2 Re(Z_{e1}) Re(Z_{e0}), \quad (25)$$

where P_{IF} is the power dissipated in the IF load and P_{RF} is the available power from the source.

B. Calculations

Tables I and II show the assumed and calculated diode parameters, respectively, and Table III indicates the non-zero embedding impedances assumed for the conversion loss calculations. The broadband assumption was used, that is, the impedances of the RF and the image terminations were assumed equal. According to an analysis by Grossman [16], the input impedance of a corner cube antenna is equal to approximately 145 Ω near the RF frequency. The other embedding impedances were chosen through impedance matching considerations with the diode. We chose an IF load impedance of 250 Ω, which in most cases was close to the small signal output impedance of the diode. The LO source impedance was assumed to be 100 + j 100 Ω, to match the input impedance of a typical diode.

Table I. Diode dimensions and doping concentrations.

epilayer material	GaAs	$In_{0.2}Ga_{0.8}As$	$In_{0.53}Ga_{0.47}As$
anode diameter	0.5 μm	0.5 μm	0.5 μm
chip diameter	100 μm	100 μm	100 μm
chip thickness	125 μm	125 μm	125 μm
epilayer thickness	807 Å	655 Å	389 Å
epilayer doping	5.0×10^{17} cm^{-3}	5.0×10^{17} cm^{-3}	5.0×10^{17} cm^{-3}
substrate doping	5.0×10^{18} cm^{-3}	5.0×10^{18} cm^{-3}	5.0×10^{18} cm^{-3}

Table II. Predicted diode parameters.

epilayer material	GaAs	$In_{0.2}Ga_{0.8}As$	$In_{0.53}Ga_{0.47}As$
C_{jo}	0.56 fF	0.67 fF	1.13 fF
R_s at 1THz	23.3 Ω	17.3 Ω	13.0 Ω
X_s at 1THz	18.8 Ω	16.0 Ω	12.2 Ω
I_{sat}	1.16×10^{-16} A	2.06×10^{-11} A	1.07×10^{-5} A
I_{max}	0.70×10^{-3} A	0.70×10^{-3} A	0.70×10^{-3} A
η	1.152	1.184	1.271

Table III. Mixer embedding impedances.

ω_{RF}	145 Ω
ω_{image}	145 Ω
ω_{LO}	100 + j 100 Ω
ω_{IF}	250 Ω

Figure 8 indicates the predicted conversion loss, as a function of V_{LO}, for a whisker-contacted GaAs diode. In general, the conversion loss decreases as the LO voltage is increased. Also, the LO voltage (and therefore power) requirement can be reduced by biasing the diode. Figure 9 shows the predicted conversion loss of various un-biased InGaAs and GaAs diodes. It is highly significant that the minimum conversion loss of $In_{0.53}Ga_{0.47}As$ diodes is only 1 to 2 dB greater than that of GaAs diodes. The much greater saturation current of $In_{0.53}Ga_{0.47}As$ diodes is not expected to significantly degrade their performance vis-a-vis GaAs diodes. Of even greater importance is that they will achieve this performance with only one-fourth of the LO voltage as required by GaAs diodes. The corresponding LO power requirement for $In_{0.53}Ga_{0.47}As$ diodes is about 0.1 mW, one-sixteenth that of GaAs diodes.

We also calculated the conversion loss of a sub-harmonically pumped, anti-parallel, whisker-contacted diode pair, operated without bias voltages. We caution that this is a preliminary analysis that was done before we performed the more accurate I-V analysis using the Crowell-Sze-Chang model, and therefore the predictions cannot be precisely compared with those of single diodes. To perform the conversion loss analysis, we used the single-diode equivalent circuit, in which the anti-parallel pair is modeled as a single diode in a mixer with twice the embedding impedance at even harmonics, and zero embedding impedance at odd harmonics [6]. Figure 10 shows that is possible to achieve a minimum conversion loss of 10 dB or better for all of the diodes by using sufficient LO power. However, to achieve this performance, a GaAs diode requires about 0.8 mW of LO power, compared to 0.5 mW for an $In_{0.2}Ga_{0.8}As$ diode and 0.1 mW for an $In_{0.53}Ga_{0.47}As$ diode.

These predictions are especially noteworthy because the proposed anti-parallel, sub-harmonically pumped diode structure is very difficult to bias, and because obtaining sufficient LO power at frequencies in the 600 GHz to 1 THz range has been a major limitation of Schottky diode mixer performance. Therefore, with their ability to provide good conversion efficiency using LO sources of modest power, at roughly half the RF frequency, sub-harmonically pumped, anti-parallel $In_{0.53}Ga_{0.47}As$ diode mixers will offer significant performance advantages to those using GaAs diodes.

IV. Experimental Results

The objective of this facet of our work is to develop a device fabrication technology which will enable us to produce $In_xGa_{1-x}As$ mixer diodes with predictable electrical characteristics. This was implemented by fabricating several batches of $In_xGa_{1-x}As$ diodes and comparing their DC characteristics with those of nearly equivalent GaAs diodes.

A. Fabrication Technology

In order to proceed with the fabrication of initial devices while the aforementioned theoretical analysis was being carried out, a simple model was used to estimate the diode performance for various values of indium mole fraction, x. Based on the lumped element diode model, the device impedance in the low conductivity state, Z_{off}, and the impedance in the high conductivity state, Z_{on}, were calculated in order to estimate the ratio Z_{off}/Z_{on}, which is infinite in the ideal case. We imposed a minimum allowable value of $Z_{off}/Z_{on} = 100$; this lead to preliminary values of $x = 0.2$ and $N_D = 2x10^{17}$ cm^{-3}. It was felt at the time that the significant leakage current predicted for $In_{0.53}Ga_{0.47}As$ devices would degrade mixer performance seriously; thus a lower mole fraction was chosen for our initial fabrication work. Unfortunately, $In_{0.2}Ga_{0.8}As$ is not lattice matched to any known usable substrate; therefore it was grown on GaAs, which presents the closest lattice match.

Whisker-contacted Schottky diodes were fabricated on $In_xGa_{1-x}As$ using virtually the same processing steps as are employed in the fabrication of GaAs diodes. They are as follows:

1. Active Layer Thinning. The active layer of the InGaAs is intentionally grown thicker than required for device fabrication. This allows impurity concentration profiling by a standard C(V) technique. The active layer is subsequently thinned electrochemically to a

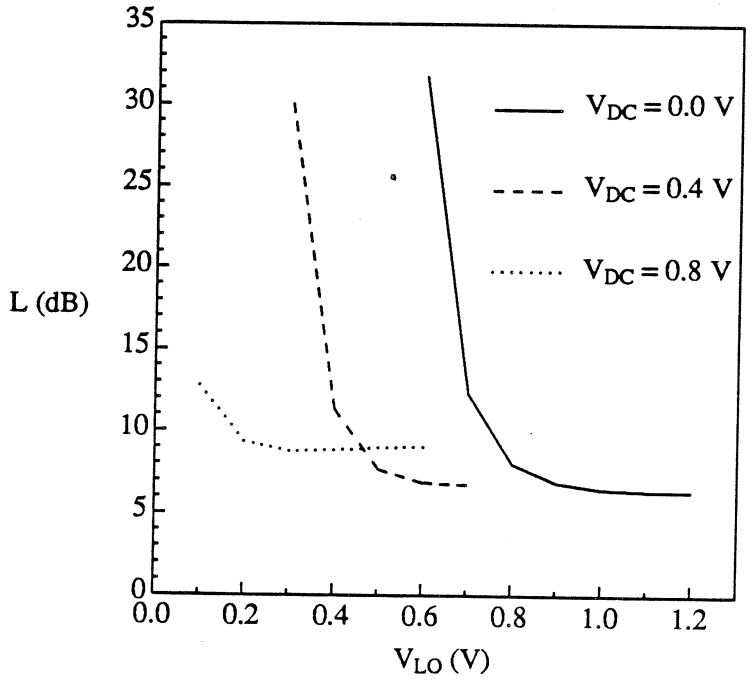

Figure 8. Predicted conversion loss of GaAs Schottky diode mixers at various bias at f_{LO} = 1 THz. Diode and mixer parameters are given in Tables I - III.

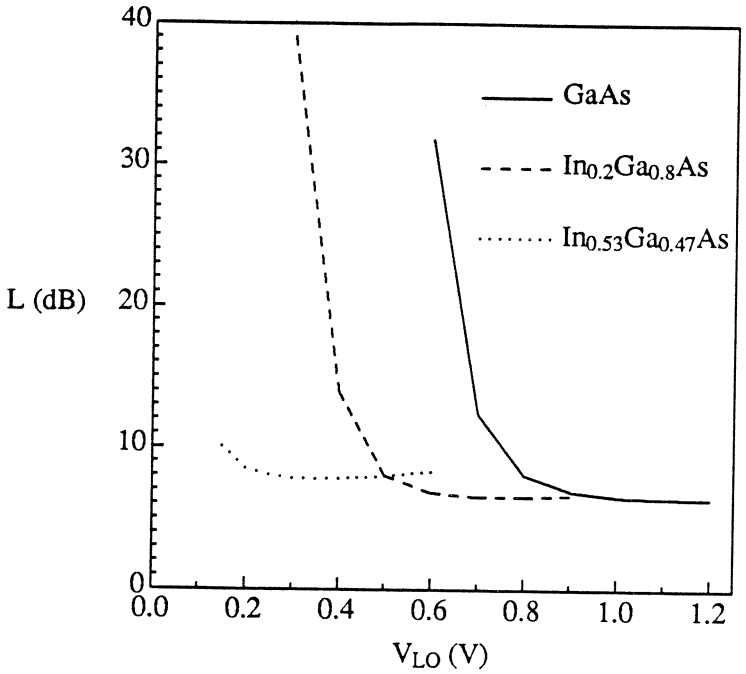

Figure 9. Predicted conversion loss of various single diode mixers at zero bias at f_{LO} = 1 THz.

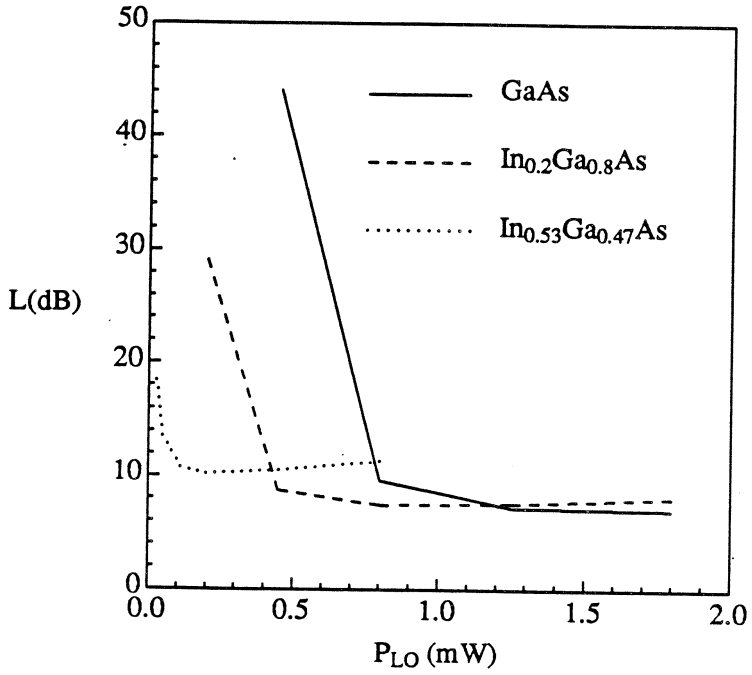

Figure 10. Predicted conversion loss of various anti-parallel, sub-harmonically pumped mixers at f_{LO} = 500 GHz and f_{RF} = 1005 GHz.

thickness slightly greater than the zero-bias depletion depth.

2. Oxide Deposition. A thin (4200 A) layer of SiO_2 is pyrolitically deposited on the active layer. This serves to not only passivate the resulting devices but also as an anode definition mask.

3. Anode Definition. Standard photolithography and reactive ion etching are employed to define anode windows in the SiO_2 layer. Anode metals (Pt and Au) are electroplated through these windows onto the underlying active semiconductor material to form the device anodes.

4. Ohmic Contact Formation. For back-contact devices, the n^{++} substrate is thinned mechanically and an ohmic contact is formed by electroplating Sn-Ni/Ni/Au and subsequent alloying at 425 °C.

Due to the lattice mismatch between the $In_{0.2}Ga_{0.8}As$ active layer and the GaAs substrate, cross-hatching was evident (as expected) on the surface, however it was observed to be minimal in samples which included a graded region from x = 0 to x = 0.2. The non-uniformity of the surface was manifested in the SiO_2 layer as well, but did not significantly hamper the fabrication procedure.

The most crucial step in device fabrication is anode formation. The detail of this step is specific to the semiconductor material and metal used. Early attempts at anode formation on $In_xGa_{1-x}As$ resulted in a device current-voltage characteristic which was changed, often irreversibly, by the application of high forward current. (This phenomenon is termed diode creep.) In addition, I-V characteristics varied greatly from device-to-device on the same 10 mil x 10 mil chip. These problems were ultimately overcome by slight adjustments of the processing parameters.

B. Measured Diode Characteristics

$In_xGa_{1-x}As$ diodes, as expected, have a lower forward turn-on voltage than do corresponding GaAs devices. This is illustrated in Fig. 11 which shows the actual I-V characteristics of both an $In_{0.2}Ga_{0.8}As$

diode and a GaAs diode. The difference in diode turn-on sharpness is due to differences in the active layer dopings, which is related to the ideality factor.

Figure 12 shows an I-V plot of data measured for four diodes with varying indium mole fractions. Diode 1T2/30 was fabricated on GaAs, while the others were fabricated on $In_xGa_{1-x}As$. Diode SDL33/1/5 has x = 0.3, and SDL25/3/5 and QED1/11/3 have x = 0.2. The straight lines represent the best fit through the three "low current" points, i.e., 100 nA, 1 μA, and 10 μA, where the characteristic is very nearly linear. The series resistance for each diode was inferred from the distance between that line and the measured voltage at a current of 1 mA. It can be noted that all of the devices have nearly the same ideality factor in that "low current" region.

C. Analysis

The device physical and electrical parameters are listed in Table IV. The first column lists the diode identification number; the next three columns indicate values of the indium mole fraction, active layer doping, and thickness, as specified to the material supplier. The diameters of the anodes were inferred from the measured zero-bias capacitance, and are listed in the fifth column.[2] The remaining columns contain values obtained from the measurement of the DC or low frequency characteristics of each diode. The voltage measured due to a bias of 10 μA, which is designated in the table as $V_{10\mu A}$, is listed for each device for comparison purposes.

Table IV shows that in devices with approximately the same epilayer thicknesses (within 200 A), R_s for the $In_xGa_{1-x}As$ devices is significantly less than that for the GaAs diode. This is due primarily to two factors: the larger diameter anodes of the InGaAs devices and the higher electron mobility of InGaAs. The other InGaAs devices, which have a thicker epilayer and lower doping than the GaAs diode, have relatively large R_s values. The capacitance values of the InGaAs diodes are greater than that of the GaAs diodes due to their greater device area. Their larger anode diameters were not intentional, but occurred due to the non-optimization of our initial processing parameters.

As was previously noted, all of the diodes have similar measured values of the ideality factor. The breakdown voltages, as expected [17], decrease with decreasing values of the energy gap, that is, with increasing values of x. Note that V_{BR} also depends on the epilayer thickness and doping, which accounts for V_{BR} of SDL25/3/5 being greater than that of the GaAs diode, in spite of its smaller energy gap.

The voltages measured at a current of 10 μA clearly indicate that the InGaAs devices require a substantially smaller voltage to achieve the same current density as the GaAs diode. It is this property of InGaAs that will be exploited in the anti-parallel configuration.

V. Conclusion

The difficulty of obtaining sufficient LO power from solid-state sources at frequencies above 600 GHz has become a limiting factor in the design and operation of heterodyne receivers in that frequency range. One method of circumventing the problem is to employ sub-harmonic mixing, which requires power at about half the frequency of the RF signal. The simplest configuration that relies on sub-harmonic pumping uses two anti-parallel diodes. However, GaAs diodes used in such an arrangement require a substantial bias for optimum conversion performance, and it is quite difficult to bias diodes in this configuration. We have therefore proposed the use of InGaAs mixer diodes, which have a low turn-on voltage, and can therefore efficiently operate without DC bias. The $In_xGa_{1-x}As$ material system allows for a controllable lowering of the Schottky barrier height and a corresponding reduction in turn-on voltage. Our work here has focused on both theoretical studies of the conversion performance and experimental development of InGaAs Schottky diodes. The theoretical studies have included the

[2] We note that the diameters listed here are greater than the diameters of the diodes in the 1 THz simulations discussed in the preceding two sections.

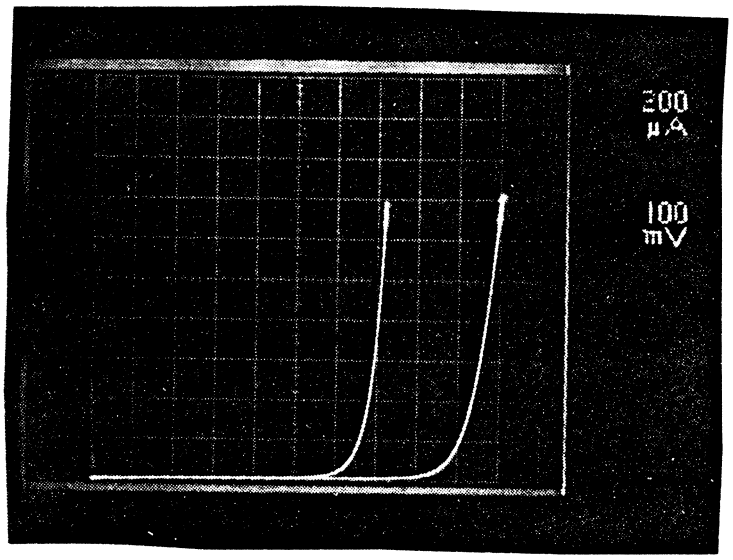

Figure 11. A comparison of the I-V characteristics of an $In_{0.2}Ga_{0.8}As$ diode (left-most trace) and a GaAs diode.

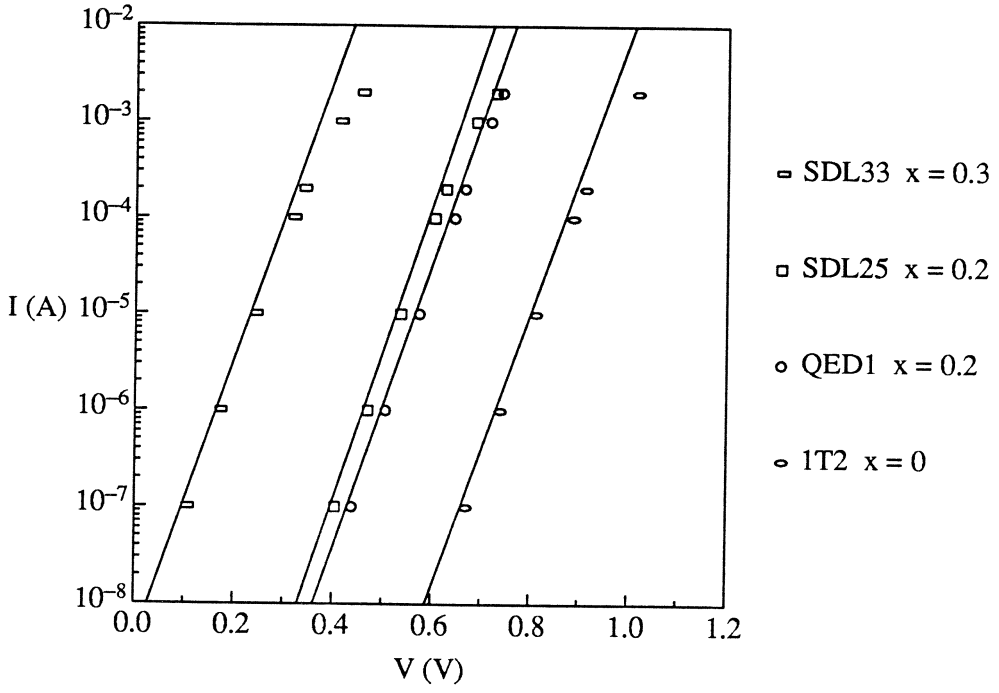

Figure 12. Current-voltage plot of four diodes with the indicated indium mole fractions.

Table IV. Measured and specified diode parameters.

Diode	x	N_D (cm^{-3})	t_{epi} (A)	d (μm)	R_s (Ω)	C_{jo} (fF)	η	V_{BR} (V)	$V_{10\mu A}$ (mV)
1T2/30	0.0	4×10^{17}	1000	0.97	20.5	0.95	1.21	5.8	799.8
SDL25/3/5	0.2	1.3×10^{17}	1500	1.3	22.0	2.16	1.11	7.3	525.6
QED1/11/3	0.2	2×10^{17}	800	1.5	10.5	3.10	1.15	4.1	564.2
QED2/11/2	0.2	2×10^{17}	800	1.5	11.0	3.42	1.15	4.2	569.1
SDL33/1/5	0.3	2×10^{17}	1500	1.3	27.0	2.34	1.19	< 1	232.3

prediction of diode parameters as well as the study of conversion loss and LO power requirements of InGaAs diodes.

Our studies of the diode characteristics have centered on the RF series resistance, an important parasitic, and the current-voltage relationship. We have performed calculations of the RF series resistance using a finite difference technique that considers high frequency phenomena such as the skin effect and charge carrier inertia. The calculations indicate that the series resistance of these devices will be lower than that of conventional GaAs devices, and thereby reduce the conversion loss. We have also written a program to predict the current-voltage relationship of Schottky diodes. Our program uses the model of Crowell, Chang and Sze, and takes into consideration quantum-mechanical reflection and image force lowering of the Schottky barrier. The results indicate that $In_{0.53}Ga_{0.47}As$ will have a much lower turn-on voltage than GaAs diodes, as expected. More importantly, the ideality factor of these diodes will be only slightly greater than that of GaAs diodes.

We have performed conversion loss studies of single and anti-parallel diode mixers using a computer program by Maas, modified for the more sophisticated I-V relationship discussed above. The results indicate that unbiased $In_{0.53}Ga_{0.47}As$ diodes will require about one-sixteenth of the LO power required by GaAs diodes, and will have an optimum conversion loss within 1 to 2 dB of comparably sized GaAs diodes. Simulations of sub-harmonically pumped, anti-parallel diodes have produced similar results.

In addition to the theoretical investigations, we have refined fabrication technology so that InGaAs diodes with stable, predictable electrical characteristics can be reproduced reliably. Initial problems with the electrical stability of devices were resolved by small modifications to the processing parameters; however, some optimization remains to be completed. Our results obtained thus far agree well with our I-V model and indicate that InGaAs devices can match or exceed the performance of GaAs diodes in terms of series resistance and the slope of the current-voltage characteristic.

This work is continuing with the investigation of $In_{0.53}Ga_{0.47}As$ diodes on InP substrates, in both the whisker-contacted and planar anti-parallel configurations. Additional variations to the fabrication procedure are anticipated for material with indium mole fraction greater than about 0.3, and although the changes are expected to be relatively minor, the optimization process will have to be repeated to ensure reliable reproducibility. DC and RF testing will be performed on the new devices to determine how well our model predicts device behavior.

Acknowledgments

We would like to thank Drs. J. East and G. Haddad of the University of Michigan Center for Space Terahertz Technology for their guidance and many helpful suggestions.

REFERENCES

[1] C.R. Crowell and S.M. Sze, "Quantum-Mechanical Reflection of Electrons at Metal-Semiconductors Barriers: Electron Transport in Semiconductor-Metal-Semiconductor Structures," *Journal of Applied Physics*, Vol. 37, No. 7, June 1966, pp. 2683-2689.

[2] C.Y. Chang and S.M. Sze, "Carrier Transport Across Metal-Semiconductor Barriers," *Solid-State Electronics*, Vol. 13, pp. 727-740.

[3] U.V. Bhapkar, "An Investigation of the Series Impedance of GaAs Schottky Barrier Diodes," M.S. Thesis, University of Virginia, May 1990.

[4] A.R. Kerr, "A Technique for Determining the Local Oscillator Waveforms in a Microwave Mixer," *IEEE Transactions*, Vol. MTT-23, Oct. 1975, pp. 828-831.

[5] D.N. Held and A.R. Kerr, "Conversion Loss and Noise of Microwave and Millimeter-Wave Mixers: Part I -- Theory," *IEEE Transactions*, Vol. MTT-26, Feb. 1978, pp. 49-55.

[6] S.A. Maas, *Microwave Mixers*, Artech House, 1986, pp. 89-128, pp. 315-339.

[7] K. Kajiyama, Y. Mizushima, and S. Sakata, "Schottky Barrier Height of n–$In_xGa_{1-x}As$ Diodes," *Applied Physics Letters*, Vol. 23, No. 8, 15 Oct. 1973, pp. 458-459.

[8] J.A. Copeland, "Diode Edge Effects of Doping-Profile Measurements," *IEEE Transactions*, Vol. ED-17, No. 4, May 1979, pp. 404-407.

[9] L.E. Dickens, "Spreading Resistance as a Function of Frequency," *IEEE Transactions*, Vol. MTT-15, No. 2, Feb. 1967, pp. 101-109.

[10] S.M. Sze, *Physics of Semiconductor Devices*, 2nd Ed., Wiley-Interscience, 1981, p. 29.

[11] Sze, p. 849.

[12] J. Costa, A.Peczalski, and M. Shur, "Monte Carlo Studies of Steady-State Electronic Transport in Compensated $In_{0.53}$GaSub0.47As," *Journal of Applied Physics*, Vol. 65, No. 12, 15 June 1989, pp. 5205-5206.

[13] E.H.C. Parker, *The Technology and Physics of Molecular Beam Epitaxy*, Plenum Press, p. 129.

[14] Sze, pp. 255-257.

[15] F.A. Padovani and R. Stratton, "Field and Thermionic-Field Emission in Schottky Barriers," *Solid State Electronics*, Vol. 9, 1966, pp. 695-707.

[16] E.N. Grossman, "The Performance of Schottky Diodes as Far-Infrared Modulators," *Int. Journal on Infrared and Millimeter Waves*, Vol. 8, No. 10, 1987, pp. 1293-13.

[17] Sze, p. 104.